

Infrared spectra and ab initio calculations of the matrix isolated $(\text{CO}_2) \cdot (\text{H}_2\text{SO}_4)$ and $(\text{CO}_2) \cdot (\text{SO}_3)$ complexes

Aharon Givan^a, Aharon Loewenschuss^{a,*}, Claus J. Nielsen^b

^aDepartment of Inorganic and Analytical Chemistry, The Hebrew University of Jerusalem, Jerusalem 91904, Israel

^bDepartment of Chemistry, University of Oslo, Blindern, N-0315 Oslo, Norway

Received 18 April 2001; accepted 8 May 2001

Abstract

In Ar/CO₂/H₂SO₄ layers deposited at 15–18 K, infrared bands originating in the $(\text{CO}_2) \cdot (\text{H}_2\text{SO}_4)$ and $(\text{CO}_2) \cdot (\text{SO}_3)$ complexes were identified. The complexes were found to be produced predominantly during the matrix deposition process. Ab initio calculations on these complexes are presented and compared with the experimental results. The $(\text{CO}_2) \cdot (\text{H}_2\text{SO}_4)$ complex is formed by an end-on O=C=O...HO interaction. The $(\text{CO}_2) \cdot (\text{SO}_3)$ interaction occurs mainly via an interaction between the O atom of CO₂ and the S atom of SO₃ and a secondary interaction between the C atom of CO₂ and the most adjacent O atom of SO₃. © 2002 Elsevier Science B.V. All rights reserved.

Keywords: Sulfuric acid complexes; Matrix isolation spectroscopy; Infrared spectroscopy; Ab initio calculations

1. Introduction

Sulfuric acid is an important atmospheric species found in significant abundance in polar stratospheric clouds and in low temperature sub-micron aerosol drops [1]. In several recent studies we investigated the infrared spectra of pure H₂SO₄ [2] and D₂SO₄ [3] vapors (containing SO₃ and H₂O/D₂O in equilibrium concentrations) trapped in solid argon matrices along with the relevant ab initio calculations of both the structure and vibrational frequencies. We also reported the infrared spectra of molecular complexes of H₂SO₄ — its dimer [2] and its adducts with atmospheric species like H₂O [2], CO [4], N₂, NO and N₂O₂ [5] and HCl [6] isolated in solid argon. Several vibra-

tional bands of the mixed (L)·(H₂O)·(H₂SO₄) complexes [4,5] were also identified, leading to an understanding of their bonding scheme. The inevitable presence, due to chemical equilibrium, of SO₃ in the sulfuric-acid/argon matrix samples, also facilitated the assignment of infrared features of the (SO₃)₂ [2], (OC)·(SO₃) [4] and the, much weaker, (N₂)·(SO₃) [5] species. However, no evidence was found for the stabilization of the parallel complexes of SO₃ with H₂O, NO and with N₂O₂ in solid argon, although other studies reported the existence of stable (H₂O)_{1–2}·(SO₃) molecular complexes in nitrogen [7] and oxygen [8] solids. The spectral results indicated that attachment of CO, N₂, NO, N₂O₂ and HCl to the H₂SO₄ moiety occurs through hydrogen bonding to the O–H moiety of H₂SO₄ (HCl has a secondary link to the S=O₂ oxygen [6]), whereas the OC...SO₃ interaction occurs via the respective C and S atoms. The molecular species stabilized in solid argon samples were shown to essentially originate in the

* Corresponding author. Tel.: +972-2-658-5313;
fax: +972-2-658-5319.

E-mail address: loewena@chem.ch.huji.ac.il
(A. Loewenschuss).

low temperature deposition process rather than to represent a gas phase equilibrium. The present communication reports the infrared spectrum of the H_2SO_4 and SO_3 complexes with another abundant atmospheric constituent, CO_2 , along with the relevant *ab initio* calculations. We found no previous reports on spectroscopic evidence for the existence of this complex.

2. Experimental

Sulfuric acid was supplied by Prolabo (p. A.), the Ar (5.7 by AGA). Carbon dioxide impurities produced the relevant complexes. Experimental details were given previously [2–6]. In short, H_2SO_4 vapors for deposition were taken from a drop of sulfuric acid placed in a furnace consisting of a quartz tube ending in a nozzle, wrapped by a heating coil. Gaseous CO_2 /Ar mixtures (with estimated 1:25–1:500 ratios) were either passed through the H_2SO_4 containing nozzle (warmed to a maximum of 38°C), or, the two components were sprayed separately onto a 5 K CsI window. Cooling was achieved by an Air Products HS-4 Heliplex cryostat employing two HC-4 MK 1 compressor modules. Temperatures were controlled by a Lake Shore model 330 temperature controller using Si diode sensors. Typical deposition times were of 1–4 h depending upon sample dilutions, while deposition rates were of several mmol h^{-1} . Temperature cycling of the samples was conducted by a slow warming (1 K min^{-1}) up to 38 K, followed by quick recooling to 5 K. Infrared spectra were recorded on Bruker IFS 88 and Bruker IFS 66 FTIR spectrometers, employing DTGS detectors and coadding 32–128 scans, at resolutions of $0.25\text{--}2 \text{ cm}^{-1}$.

3. Quantum chemical and normal mode computations

The *ab initio* calculations were carried out using the GAUSSIAN 98 suite of programs [9]. The standard structure optimization consisted of a DFT calculation using the B3LYP functional [10] and the medium-sized cc-pVDZ basis set, which includes polarization functions. Additional DFT and MP2 calculations were carried out with the cc-pVTZ, cc-pVQZ, and with the

augmented cc-pVDZ and cc-pVTZ basis sets — that is, basis sets including diffuse functions.

The Basis Set Superposition Error (BSSE) was assessed by the Counterpoise (CP) Correction [11]. The complex energy minus the monomer energies is the directly calculated complexation energy.

$$\Delta E_{\text{complex}} = E(\text{AB})_{\text{ab}}^* - E(\text{A})_{\text{a}} - E(\text{B})_{\text{b}},$$

$$\Delta E_{\text{CP}} = E(\text{A})_{\text{ab}}^* - E(\text{A})_{\text{a}}^* + E(\text{B})_{\text{ab}}^* - E(\text{B})_{\text{b}}^*$$

where the asterisk (*) denotes the structure of the complex and the subscripts a and b the basis functions of the monomers A and B, respectively. The counterpoise corrected energy of complexation is given as $\Delta E_{\text{complex}} - \Delta E_{\text{CP}}$.

The normal mode calculations were carried out with the VIBROT and FLINDA programs [12], which utilize the cartesian force constants calculated by Gaussian and transform them to internal valence co-ordinates. The programs include the option to scale the valence co-ordinate force field according to $F_{ij}^{\text{scaled}} = \sqrt{\alpha_i \alpha_j} F_{ij}$, where α_i and α_j are scaling factors for the internal co-ordinates *i* and *j*, respectively.

4. Results and discussion

Due to the inherent equilibrium, the vapor phase of sulfuric acid and consequently matrix isolated samples of these vapors, contain, in addition to sulfuric acid molecules, significant amounts of SO_3 and H_2O [2]. Due to its higher mobility, the latter is the dominant partner to complex formation in the matrix. Therefore, only at relatively high CO_2 /sulfuric acid ratios in the Ar/ CO_2 / H_2SO_4 deposits, can the CO_2 molecules in the matrix both trap a large percentage of the water molecules to produce $(\text{CO}_2) \cdot (\text{H}_2\text{O})$ species as well as combine with the, now higher, fraction of free sulfuric acid molecules to form a $(\text{CO}_2) \cdot (\text{H}_2\text{SO}_4)$ complex. Spectral identification of the latter complex was, therefore, possible only for samples with concentration ratios of $\text{CO}_2/\text{Ar} \geq 2\%$.

Since bands recorded in the present work for CO_2 free samples were discussed previously [2,3], and attributed to species like H_2SO_4 , H_2O , SO_3 , their dimers, polymers and their intermolecular complexes, only absorptions showing a dependence on the CO_2

Table 1

Vibrational band positions (cm^{-1}) and assignment of CO_2 containing species in deposited $\text{Ar}/\text{CO}_2/\text{H}_2\text{SO}_4$ layers ((s) strong, (m) medium, (w) weak, (sh) shoulder, (br) broad)

| Bands | Assignment |
|--------------------------|---|
| 3726 (s) | $\nu_3(\text{H}_2\text{O})$ in $(\text{H}_2\text{O})\cdot(\text{CO}_2)$ |
| 3694, 3680 (br) | $\nu_3(\text{H}_2\text{O})$ in $(\text{H}_2\text{O})_m\cdot(\text{CO}_2)_n$ polymers |
| 3638 (w) | $\nu_1(\text{H}_2\text{O})$ in $(\text{H}_2\text{O})\cdot(\text{CO}_2)$ |
| 3500 (m, sh) | $\nu_9(\text{b})$ OH antisymmetric stretch of $(\text{CO}_2)\cdot(\text{H}_2\text{SO}_4)$ |
| 2348.2 (w) | $\nu_3(\text{CO}_2)$ in $(\text{CO}_2)\cdot(\text{H}_2\text{SO}_4)$ |
| 2346.8 (m) | $\nu_3(\text{CO}_2)$ in $(\text{H}_2\text{O})\cdot(\text{CO}_2)$ |
| 2344.8 (vs) | $\nu_3(\text{CO}_2)$ |
| 1601 (br) | $\nu_2(\text{H}_2\text{O})$ in $(\text{H}_2\text{O})_m\cdot(\text{CO}_2)_n$ polymers |
| 1598 (s) | $\nu_2(\text{H}_2\text{O})$ in $(\text{H}_2\text{O})\cdot(\text{CO}_2)$ |
| 1445.5 (s) | $\nu_{10}(\text{b})$ $\text{S}=\text{O}_2$ stretch of $(\text{CO}_2)\cdot(\text{H}_2\text{SO}_4)$ |
| 1435 (br) | $\text{S}=\text{O}_2$ antisymmetric stretch of $(\text{CO}_2)_m\cdot(\text{H}_2\text{O})_n\cdot(\text{H}_2\text{SO}_4)_p$ polymers |
| 1398.2 (s) 1395.3 (s) | $\nu_3(\text{e}')$ of SO_3 stretch of $(\text{CO}_2)\cdot(\text{SO}_3)$ |
| 1213.6 (s) | $\nu_2(\text{a})$ $\text{S}=\text{O}_2$ stretch of $(\text{CO}_2)\cdot(\text{H}_2\text{SO}_4)$ |
| 1172 (br) | $\text{S}=\text{O}_2$ symmetric stretch of $(\text{CO}_2)_m\cdot(\text{H}_2\text{O})_n\cdot(\text{H}_2\text{SO}_4)_p$ polymers |
| 908 (br) | $\text{S}-(\text{OH})_2$ antisymmetric stretch of $(\text{CO}_2)_m\cdot(\text{H}_2\text{O})_n\cdot(\text{H}_2\text{SO}_4)_p$ polymers |
| 894.8 (s) | $\nu_{12}(\text{b})$ $\text{S}-(\text{OH})_2$ stretch of $(\text{CO}_2)\cdot(\text{H}_2\text{SO}_4)$ |
| 849.7 (br) | $\text{S}-(\text{OH})_2$ symmetric stretch of $(\text{CO}_2)_m\cdot(\text{H}_2\text{O})_n\cdot(\text{H}_2\text{SO}_4)_p$ polymers |
| 841.1 (s) | $\nu_4(\text{a})$ $\text{S}-(\text{OH})_2$ stretch of $(\text{CO}_2)\cdot(\text{H}_2\text{SO}_4)$ |
| 662.6 (s) {662.4; 663.5} | $\nu_2(\text{H}_2\text{O})\cdot(\text{CO}_2)$ and $\nu_2(\text{CO}_2)$ |
| 565 (br) | $\text{S}=\text{O}_2$ rock of $(\text{CO}_2)_m\cdot(\text{H}_2\text{O})_n\cdot(\text{H}_2\text{SO}_4)_p$ polymers |
| 561.4 (m) | $\nu_{13}(\text{b})$ $\text{S}=\text{O}_2$ rock of $(\text{CO}_2)\cdot(\text{H}_2\text{SO}_4)$ |
| 553 (br) | $\text{S}=\text{O}_2$ bend of $(\text{CO}_2)_m\cdot(\text{H}_2\text{O})_n\cdot(\text{H}_2\text{SO}_4)_p$ polymers |
| 551.4 (s) | $\nu_5(\text{a})$ $\text{S}=\text{O}_2$ bend of $(\text{CO}_2)\cdot(\text{H}_2\text{SO}_4)$ |
| 531.6 (s) | $\nu_4(\text{e}')$ bend of $(\text{CO}_2)\cdot(\text{SO}_3)$ |
| 488.6 (s) | $\nu_2(\text{a}''_2)$ bend of $(\text{CO}_2)\cdot(\text{SO}_3)$ |
| 478.5 (br) | ν_2 bend of $(\text{CO}_2)_m\cdot(\text{H}_2\text{O})_n\cdot(\text{SO}_3)_p$ polymers |

concentration will be related to in the following discussion and are summarized in Table 1. The experiments that demonstrated the clearest complexation with CO_2 , were those conducted at higher temperatures (15–18 K). However, the samples produced at elevated temperatures, may also be expected to contain considerable amounts of polymeric species, especially such involving water molecules, the most mobile species in these layers. The spectral bands of these polymeric species are included in Table 1, but are not discussed further.

4.1. The 1:1 $(\text{CO}_2)\cdot(\text{H}_2\text{SO}_4)$ complex

The absorption bands assigned to the 1:1 $(\text{CO}_2)\cdot(\text{H}_2\text{SO}_4)$ complex are compiled in Table 2, where they are compared to those of other 1:1 $(\text{L})\cdot(\text{H}_2\text{SO}_4)$ molecular complexes studied by us ($\text{L}=\text{CO}$, N_2 , NO , N_2O_2 , HCl) [4–6], along with the respective spectral shifts of these bands from the relevant argon-matrix isolated H_2SO_4 monomer absorptions.

The high wavenumber spectral region, where the $\nu(\text{OH})$ stretches are active, shows a large number of bands, even for samples of matrix isolated H_2SO_4 vapors not containing any added CO_2 impurities. A representative spectrum, reproduced in trace A of Fig. 1a shows peaks attributable to monomeric H_2O vib-rotors [13], the sharp, strong 3566.7 cm^{-1} line, assigned to the antisymmetric $\nu(\text{OH})$ stretch of argon isolated H_2SO_4 [2] along with its two satellites, attributed to the $(\text{H}_2\text{O})_{1-2}\cdot(\text{H}_2\text{SO}_4)$ complexes [2] as well as absorption bands due to the water dimer (3708 cm^{-1}) and trimer (3527.8 cm^{-1} , shoulder, 3516.2 cm^{-1} [13]). Introducing CO_2 into the deposition mixture, at a concentration of about 2%, causes drastic spectral changes (Fig. 1a, trace B): the rotational bands of monomeric water disappear and a strong absorption at 3726 cm^{-1} as well as a weaker one at 3638 cm^{-1} appear. These are assigned to the $(\text{H}_2\text{O})\cdot(\text{CO}_2)$ complex, in accord with band positions in both argon and oxygen matrices [14–16]. In addition to these lines a new absorption emerges at 3500 cm^{-1} as a shoulder on the low energy side of the 3516.2 cm^{-1} water trimer band. Similar to the other CO_2 dependent spectral features, its intensity is defined already upon deposition and does not

Table 2
Vibrational modes of argon matrix isolated 1:1 (L)·(H₂SO₄) complexes, **band positions** (cm⁻¹), **shifts** (cm⁻¹) and (relative shifts %)

| Assignment | H ₂ SO ₄ /Ar ^a Ligands | | | | | |
|--|---|-----------------------------|-----------------|--|-----------------|------------------|
| | CO ₂ ^b | N ₂ ^c | NO ^e | N ₂ O ₂ ^e | OC ^d | HCl ^e |
| ν₉ (b) | 3566.7 | 3500 | 3452.3 | 3446.5 | 3371.1 | 3393 |
| OH antisymmetric stretch | -66.7 (-1.9%) | -19.7 (-0.6%) | -114.4 (-3.2%) | -120.2 (-3.4%) | -195.6 (-5.5%) | -173.7 (-4.9%) |
| ν₁₀ (b) | 1452.4 | 1445.5 | - | 1445.7 | 1448 | 1436.5 |
| S=O ₂ antisymmetric stretch | -6.9 (-0.5%) | -1.5 (-0.1%) | - | -6.7 (-0.5%) | -4.4 (-0.3%) | -16 (-1.1%) |
| ν₂ (a) | 1216.1 | 1213.6 | - | 1214.4 | 1209 | 1212 |
| S=O ₂ symmetric stretch | -2.5 (-0.2%) | - | - | -1.7 (-0.14%) | -7.1 (-0.58%) | -4.1 (-0.34%) |
| ν₁₂ (b) | 881.7 | 894.8 | 893.3 | 888.1 | 898.6 | - |
| S- (OH) ₂ | 13.1 (1.5%) | 10.3 (1.2%) | 11.6 (1.3%) | 6.4 (0.72%) | 17 (1.93%) | - |
| antisymmetric stretch | - | - | - | - | - | - |
| ν₄ (a) | 831.4 | 841.1 | 834.5 | 838.9 | 844.8 | - |
| S- (OH) ₂ symmetric stretch | 9.7 (1.2%) | 8.4 (1%) | 3.1 (0.37%) | 7.5 (0.9%) | 13.4 (1.61%) | - |
| ν₁₃ (b) | 558 | 561.4 | 560 | 555.3 | 562 | 561 |
| S=O ₂ rock | 3.4 (0.61%) | 1.5 (0.27%) | 2 (0.36%) | -2.7 (-0.48%) | 4 (0.71%) | 3 (0.54%) |
| ν₅ (a) | 548.1 | 551.4 | 552.2 | 545 | 553.2 | 549.5 |
| S=O ₂ bend | 3.3 (0.6%) | 1.7 (0.31%) | 4.1 (0.75%) | -3.1 (0.57%) | 5.1 (0.93%) | 1.4 (0.26%) |
| Ligand mode | - | 2348.2 | 1890 | 1807 | 2167.1 | 2636.5 |
| | 3.4 (0.15%) | -51 (-2.2%) | 18.1 (1%) | 30.6 (1.7%) | 28.6 (1.3%) | -233.5 (-8.1%) |

^a Ref. [2].

^b This work.

^c Ref. [5].

^d Ref. [4].

^e Ref. [6].

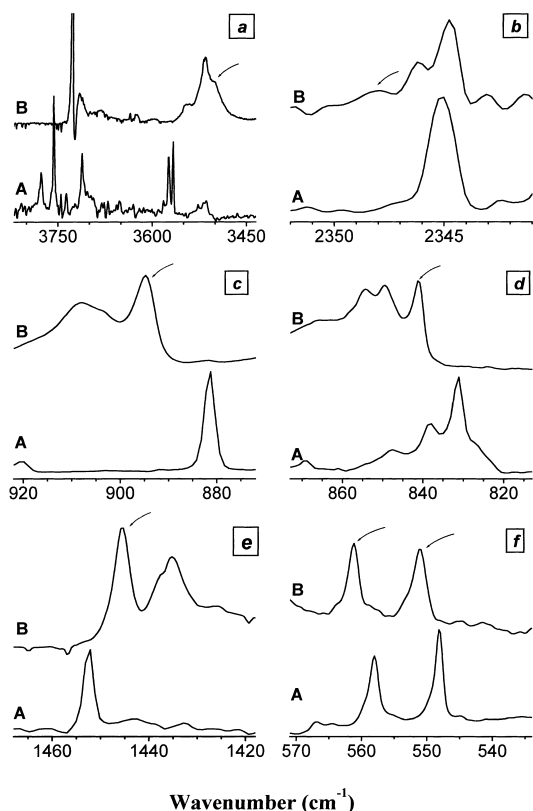


Fig. 1. Infrared vibrational bands assigned to the 1:1 $(\text{CO}_2) \cdot (\text{H}_2\text{SO}_4)$ complex in an $\text{Ar}/\text{CO}_2/\text{H}_2\text{SO}_4$ sample, deposited at 15 K. (All spectra recorded at 5 K). (a) The OH stretching mode region of H_2SO_4 ; (b) The ν_3 antisymmetric stretch mode region of CO_2 ; (c) The $\text{S}-(\text{OH})_2$ antisymmetric stretch mode region of H_2SO_4 ; (d) The $\text{S}-(\text{OH})_2$ symmetric stretch mode region of H_2SO_4 ; (e) The $\text{S}=\text{O}_2$ antisymmetric stretch of H_2SO_4 ; and (f) The $\text{S}=\text{O}_2$ rock and bend mode region of H_2SO_4 . A. $\text{Ar}/\text{CO}_2/\text{H}_2\text{SO}_4 = 200/0/1$. B. $\text{Ar}/\text{CO}_2/\text{H}_2\text{SO}_4 = 200/4/1$.

significantly change upon consequent temperature cycling. We attribute it to the bonded $\nu(\text{OH})$ stretch of the H_2SO_4 moiety in the 1:1 $(\text{CO}_2) \cdot (\text{H}_2\text{SO}_4)$ complex. The red shift (-66.7 cm^{-1} , -1.9%) of this mode from the position of the respective argon isolated free H_2SO_4 monomer band (Table 1), is the highest of all H_2SO_4 modes attributed to this species. This indicates that, in forming the complex, the CO_2 ligand gets attached to the O–H moiety of the acid.

Turning to the $\nu_3(\text{CO}_2)$ antisymmetric stretch region, we find (Fig. 1b, trace A) two sharp spectral features: a strong band at 2344.8 cm^{-1} of the argon

isolated CO_2 monomer [16], and a line of medium intensity at 2346.8 cm^{-1} , due to the $(\text{CO}_2) \cdot (\text{H}_2\text{O})$ band [14,15]. Additionally, on the blue side of this absorption another weak, broader band centered at 2348.2 cm^{-1} is observed and assigned to $\nu_3(\text{CO}_2)$ of the 1:1 $(\text{CO}_2) \cdot (\text{H}_2\text{SO}_4)$ complex.

The region of the weak $\nu_2(\text{CO}_2)$ bending mode is dominated by a rather broad absorption at 662.6 cm^{-1} , composed of the unresolved contributions of argon isolated CO_2 (663.5 cm^{-1}) and of the $(\text{CO}_2) \cdot (\text{H}_2\text{O})$ complex (662.4 cm^{-1}) [14–16]. Unlike for the CO_2 stretching mode region, we could not discern here a band clearly assignable to a 1:1 $(\text{CO}_2) \cdot (\text{H}_2\text{SO}_4)$ complex.

For the $\text{S}-(\text{OH})_2$ antisymmetric and symmetric stretching modes of the $(\text{CO}_2) \cdot (\text{H}_2\text{SO}_4)$ complex, we observed two bands at 894.8 and 841.1 cm^{-1} respectively, not found in CO_2 free samples (traces A and B of Fig. 1c and d). The above wavenumber values are blue shifted by 1.5% and 1.2%, respectively, from the parallel H_2SO_4 monomer band positions. These shifts are higher than those found, for the same vibrational modes of the H_2SO_4 complexes with N_2 , NO , and N_2O_2 , but are lower than those for the CO complex (Table 2). The higher relative shifts, due to complexation, of these modes, as compared to those of the symmetric and antisymmetric $\text{S}=\text{O}$ stretching modes, is a further confirmation that the attachment of the CO_2 ligand occurs via the $\text{S}-\text{O}-\text{H}$ moiety of the H_2SO_4 molecule.

In the $\text{S}=\text{O}$ stretching modes region, two bands, not present in the parallel $\text{H}_2\text{SO}_4/\text{Ar}$ spectra, are identified with the $(\text{CO}_2) \cdot (\text{H}_2\text{SO}_4)$ complex. The two modes active at 1445.5 cm^{-1} (antisymmetric stretch, Fig. 1e, trace B) and at 1213.6 cm^{-1} (symmetric stretch), are relatively less shifted from the respective monomeric $\text{H}_2\text{SO}_4/\text{Ar}$ bands than the bonded $\nu(\text{OH})$ stretching mode (Table 2), by a factor of 9.5–27. This is a different situation than that encountered experimentally for H_2O [2], H_2SO_4 [2] and HCl [6] and theoretically for H_2O and HCl [17], where a secondary bonding interaction between the ligand and the $\text{S}=\text{O}_2$ oxygen lone pairs was suggested.

Similarly, for the SO_4 deformation modes, recorded at 561.4 and 551.4 cm^{-1} (Fig. 1f), a red shift from the monomeric H_2SO_4 modes, of only about 0.6%, was found (Table 2).

Bonding of the $\text{O}=\text{C}=\text{O} \cdots \text{HO}-\text{SO}_2-\text{OH}$ complex

may be discussed in comparison to the analogous (OC)·(HOSO₂OH) complex studied by us [4]. CO has a low (0.13 D) dipole moment [18], the small negative charge being centered on the carbon atom [19]. Complexation with other molecules may, conceivably, occur either via the carbon atom through a C···H interaction (the (OC)·(H₂O) isomer is the more stable by theory [20]) or, alternatively, via the CO oxygen lone pairs, to produce an H···O bond. The two kinds of interaction affect opposite shifts of the ν (CO) band. The bonding via the C atom depletes electrons from the $5\sigma^*$ antibonding orbital, strengthening the CO bond and blue shifting its stretching frequency. The opposite effect is found for the bonding through the oxygen atom, which red shifts the CO stretch. Bands attributable to both isomers were indeed found experimentally for the (OC)·(H₂O) [21,22] and (OC)·(HNO₃) [23] complexes.

Following a somewhat similar line of argumentation, we note that CO₂ has a zero dipole, but a non zero quadrupole moment ($Q_M = 0.90 \text{ \AA}^2$, [14]), with the positive charge centered on the carbon atom. Thus, contrary to the case of the (CO)·(H₂SO₄) complex, bonding via the C atom would involve a *red* shift of the CO₂ stretching mode, and, alternatively, a *blue* shift for a bonding scheme involving the oxygen atoms of CO₂. As pointed out above, our experimental results are in agreement with a O=C=O···HO–SO₂–OH bonding scheme: we find a blue shift of the ν_3 (CO₂) mode along with a red shift for the ν_9 (OH) mode of sulfuric acid, indicating its involvement in an H-bond. Moreover, we obtain a logical sequence

of the ν_3 (CO₂) mode from the free CO₂ molecule at 2344.8 cm^{-1} , via the (CO₂)·(H₂O) band at 2346.8 cm^{-1} to the (CO₂)·(H₂SO₄) band at 2348.2 cm^{-1} .

The fact that complexation of CO₂ to either H₂O or H₂SO₄ indeed proceeds via its oxygens is not fully self-evident. As in the case of CO, discussed above, arguments for the alternative bonding scheme have been presented. Tso et al. [14,15] observed a splitting of the ν_2 (CO₂) bending mode band for (H₂O)·(CO₂) species trapped in oxygen matrices. This was considered in accord with the planar C_{2v} structure in which the water oxygen is connected to the CO₂ carbon, suggested by Klemperer and co-workers [24] from their microwave spectra and the results of an early ab initio calculation [25].

4.2. The 1:1 (CO₂)·(SO₃) complex

The observed band positions attributed to the fundamental modes of the (CO₂)·(SO₃) complex are listed in Table 3 and compared to the free SO₃ [2], (N₂)·(SO₃) [5], (OC)·(SO₃) [4] and the (SO₃)·(SO₃) [2] wavenumber values, all trapped in argon matrices. The new absorptions, recorded in CO₂ containing samples only are shown in Fig. 2a and b. They are assigned at 1398.2 and 1395.3 cm^{-1} , to the antisymmetric S–O stretch (originally $\nu_3(e')$), at 531.6 cm^{-1} to the in plane SO₃ bending mode (originally $\nu_4(e')$) and at 488.4 cm^{-1} to the out of plane deformation (originally $\nu_2(a''_2)$). The antisymmetric S–O stretch degeneracy is removed in the complex and its position, as well as that of the in-plane bend, are blue

Table 3

Vibrational bands (cm^{-1}) and relative shifts (%) of SO₃ in its 1:1 molecular complexes with different ligands, isolated in solid argon

| Band | SO ₃ /Ar ^a | Ligand | | | |
|----------------|----------------------------------|----------------------------------|-----------------------------|----------------------------------|------------------------------|
| | | CO ₂ ^b | N ₂ ^c | CO ^d | SO ₃ ^a |
| $\nu_3(e')$ | 1385.1 | 1398.2 (0.84%) 1395.3 (0.84%) | 1393 (0.57%) | 1396.7 (0.76%) 1394.6 (0.76%) | 1389.8 (0.3%) |
| $\nu_4(e')$ | 527.2 | 531.6 (0.86%) | 530.1 (0.5%) | 532.6 (0.83%) 530.6 (0.83%) | |
| $\nu_2(a''_2)$ | 490.3 | 488.4 (−0.39%) | 489.6 (−0.14%) | 474 (−3.3%) | 481.3 (−1.84%) |

^a Ref. [2].

^b This work.

^c Ref. [5].

^d Ref. [4].

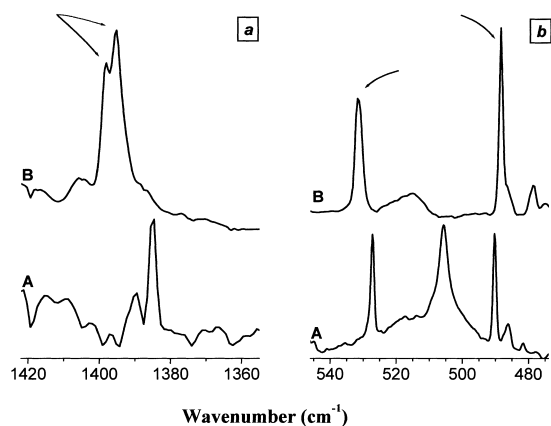


Fig. 2. Infrared vibrational bands assigned to the 1:1 $(\text{CO}_2)\cdot(\text{SO}_3)$ complex in an $\text{Ar}/\text{CO}_2/\text{H}_2\text{SO}_4$ sample, deposited at 15 K (All spectra recorded at 5 K): (a) the $\nu_3(e')$ antisymmetric stretch region of SO_3 ; and (b) the $\nu_4(e')$ antisymmetric bending and $\nu_2(a''_2)$ out of plane bending mode regions of SO_3 . A. $\text{Ar}/\text{CO}_2/\text{H}_2\text{SO}_4 = 200/0/1$. B. $\text{Ar}/\text{CO}_2/\text{H}_2\text{SO}_4 = 200/4/1$.

shifted relative to the respective free SO_3/Ar bands. A red shift is observed for the SO_3 out of plane deformation. The shifts observed for the $(\text{CO}_2)\cdot(\text{SO}_3)$ complex are larger by about a factor of two, compared to those of the very weak $(\text{N}_2)\cdot(\text{SO}_3)$ complex. Both these complexes differ significantly from the $(\text{OC})\cdot(\text{SO}_3)$ complex and the $(\text{SO}_3)_2$ dimer. In the latter, the degenerate SO_3 modes are only slightly shifted, whereas the

out-of-plane mode is red shifted by -1.8 to -3.3% , a relative shift, higher by a factor of 13.1–23.5, as compared to the $(\text{N}_2)\cdot(\text{SO}_3)$ complex and by a factor of 4.7–8.5, as compared to the $(\text{CO}_2)\cdot(\text{SO}_3)$ complex.

In SO_3 , the S atom with its strong electron affinity (empty $\pi(d)$ orbitals), is a fairly strong Lewis acid toward bases and is not oxidized by them. In the α , β , and γ - SO_3 solids [26], stable SO_3 – SO_3 bonding forms S–O–S chains, in which, each S atom is linked to four O atoms, with one of the latter forming the bridge to the next S atom. In analogy, the observed infrared band shifts of the out-of-plane deformation in complexes, suggest that SO_3 is complexed to a second SO_3 molecule or to CO, by S–O–S and C–S bonds, respectively. By this criterion of the $\nu_2(a''_2)$ shift, the $(\text{N}_2)\cdot(\text{SO}_3)$ is a much weaker and less directionally defined complex, rather close to just a neighbor–neighbor interaction. The $(\text{CO}_2)\cdot(\text{SO}_3)$ complex is somewhat stronger and its largest relative shift is found for the $\nu_3(e')$ antisymmetric stretch (Table 3). In fact, this shift is larger than that of the N_2 , CO and SO_3 complexes. This leads to the conclusion that for $(\text{CO}_2)\cdot(\text{SO}_3)$, in addition to the interaction between the sulfur atom of SO_3 and one of the CO_2 oxygens, there is an additional, secondary interaction between the C atom of CO_2 and the most adjacent oxygen of SO_3 .

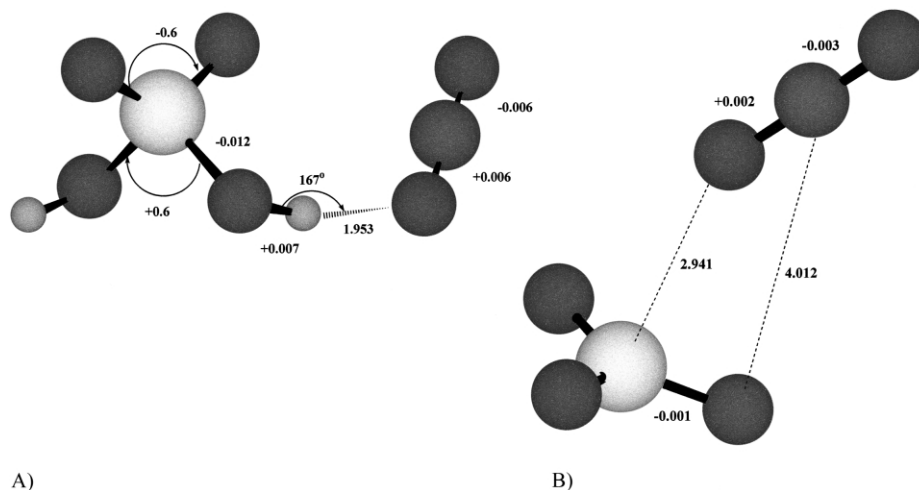


Fig. 3. B3LYP/aug-cc-pVTZ calculated structures of complexes of sulfuric acid and sulfur trioxide with the carbon dioxide molecule. Numbers are bond length (Å) and bond angle changes, relative to free monomers. A. $(\text{CO}_2)\cdot(\text{H}_2\text{SO}_4)$. B. $(\text{CO}_2)\cdot(\text{SO}_3)$. Numbers designate bond length (Å) and bond angle changes, relative to free monomers.

Table 4

B3LYP/aug-cc-pVTZ calculated vibrational frequencies and infrared intensities for H₂SO₄, CO₂ and the (CO₂)-(H₂SO₄) complex

| Monomers | | | Complex | | | Description | |
|----------------------------------|----------------|--------------------------------------|----------------------------------|--------------------------------------|---------------------------|-------------|--|
| Frequency (cm ⁻¹) | Sym. | Intensity (km mol ⁻¹) | Frequency (cm ⁻¹) | Intensity (km mol ⁻¹) | Shift (cm ⁻¹) | | |
| | | | | | Calc. | Obs. | |
| 3751.2 | A | 46 | 3751.2 | 120 | 2.1 ^a | | Free OH stretch |
| 3747.1 | B | 204 | 3615.1 | 505 | -134.0 ^a | -66.7 | Bonded OH stretch |
| 2400.4 | Σ _u | 676 | 2405.4 | 703 | 5 | 3.4 | CO ₂ antisymmetric stretch |
| 1430.2 | B | 288 | 1423.8 | 330 | -6.5 | -6.9 | S=O antisymmetric stretch |
| 1369.2 | Σ _g | 0 | 1370.1 | 4 | 1 | | CO ₂ symmetric stretch |
| 1163.4 | B | 86 | | | | | |
| 1150.7 | A | 74 | 1216.9 | 63 | 59.9 ^a | | Bonded SOH bend |
| 1185.1 | A | 163 | 1181.3 | 140 | -3.8 | -2.5 | S=O symmetric stretch |
| 1163.4 | B | 86 | | | | | |
| 1150.7 | A | 74 | 1155.7 | 97 | -1.3 ^a | | Free SOH bend |
| 839.9 | B | 322 | 853.8 | 303 | 13.9 | 13.1 | S–O antisymmetric stretch |
| 786.2 | A | 107 | 793.2 | 109 | 6.9 | 9.7 | S–O symmetric stretch |
| 673.8 | Π _u | 30 | 669.9 | 28 | -3.9 | | CO ₂ bending |
| 673.8 | Π _u | 30 | 666 | 46 | -7.8 | | CO ₂ bending |
| 530.8 | B | 22 | 534.7 | 18 | 3.9 | 3.4 | SO ₄ deformation |
| 521.3 | A | 36 | 527.3 | 65 | 6 | 3.3 | O=S=O bend |
| 306.6 | B | 56 | | | | | |
| 229.3 | A | 103 | 516.6 | 41 | 248.7 ^a | | Bonded OH torsion |
| 476.8 | B | 40 | 478.7 | 11 | 1.9 | | SO ₄ deformation |
| 417.7 | A | 13 | 397.5 | 23 | -20.2 | | SO ₄ deformation |
| 356.4 | A | 1 | 359.5 | 1 | 3.1 | | O–S–O bend |
| 306.6 | B | 56 | | | | | |
| 229.3 | A | 103 | 259 | 79 | -8.7 ^a | | Free OH torsion |
| | | | 131.5 | 3 | | | Frustrated translations and rotations |
| | | | 108.6 | 7 | | | |
| | | | 46 | 1 | | | |
| | | | 39.8 | 2 | | | |
| | | | 24.3 | 1 | | | |

^a Shift relative to the average wavenumber of the corresponding symmetric and antisymmetric modes of sulfuric acid monomer.

5. Quantum chemical calculations

To ensure that the theoretical results are not hampered by basis set deficiencies, calculations of the monomer species were also carried out at the B3LYP/cc-pVQZ level. Only minor differences were found between the results of quadruple-zeta and triple-zeta suggesting that the aug-cc-pVTZ basis set is sufficiently large and flexible to provide a reasonable description of the complexes.

The different calculations all show only one minimum on the energy surface of the (CO₂)-(H₂SO₄) complex, in which the CO₂ molecule

is linked to H₂SO₄ molecule through a hydrogen bond, S–O–H···O=C=O (Fig. 3A). The CP-corrected bonding energy and enthalpy (at 298 K), calculated at the B3LYP/cc-aug-pVTZ level, are -14.9 and -10.6 kJ mol⁻¹ respectively, which is also reflected in the rather small structural changes upon complexation (Fig. 3). We note that the hydrogen bond deviates slightly (about 12.7°) from a linear configuration. The calculated vibrational modes and infrared intensities of the complex and the isolated monomers are compared in Table 4. The Table also includes the observed calculated shifts upon complexation as well as an interpretation of the vibrations based

Table 5
Possible structures of the $(\text{CO}_2)_n(\text{SO}_3)$ complex

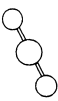
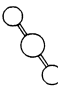
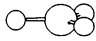
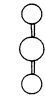





| | | | | | | | | | |
|---|---|---|---|--|---|---|---|---|---|
| |  |  |  |  |  |  |  |  |  |
| Symmetry | C_s | C_s | C_{3v} | C_{2v} | C_{2v} | C_{2v} | C_{2v} | C_{2v} | C_{2v} |
| Bonding | $\text{S} \cdots \text{O}(\text{O} \cdots \text{C})$ | $\text{S} \cdots \text{O}(\text{O} \cdots \text{C} \cdots \text{O})$ | $\text{S} \cdots \text{O}$ | $\text{O} \cdots \text{C}$ | $\text{O} \cdots \text{C}$ | $\text{O} \cdots \text{C}$ | $\text{O} \cdots \text{C} \cdots \text{O}$ | $\text{O} \cdots \text{C} \cdots \text{O}$ | $\text{O} \cdots \text{C} \cdots \text{O}$ |
| Hessian matrix | Positive definite | Negative eigenvalues | Negative eigenvalues | Negative eigenvalues | Negative eigenvalues | Negative eigenvalues | Negative eigenvalue | Negative eigenvalue | Negative eigenvalue |
| Relative energy (kJ mol^{-1}) B3LYP/ aug-cc-pVDZ | 0.0 | 0.7 | > 0.1 | 6.3 | 5.4 | 5.4 | 5.4 | 5.4 | 5.4 |
| Relative energy (kJ mol^{-1}) B3LYP/ aug-cc-pVTZ | 0.0 | 0.5 | > 0.1 | 6.0 | 5.2 | 5.2 | 5.4 | 5.4 | 5.4 |
| Relative energy (kJ mol^{-1}) MP2/aug- cc-pVDZ | 0.0 | 0.3 | 0.5 | 10.1 | 8.9 | 8.9 | 5.4 | 5.4 | 5.4 |

Table 6

B3LYP/aug-cc-pVTZ calculated vibrational frequencies and infrared intensities for SO₃, CO₂ and the (CO₂)·(SO₃) complex

| Monomers | | | Complex | | | | Description | |
|-----------------------------|------------------|----------------------------------|-----------------------------|------|----------------------------------|-------------------------|-------------|---------------------------------------|
| Frequency /cm ⁻¹ | Sym. | Intensity /km mole ⁻¹ | Frequency /cm ⁻¹ | Sym. | Intensity /km mole ⁻¹ | Shift /cm ⁻¹ | | |
| | | | | | | Calc. | Obs. | |
| 2400.4 | Σ _u | 676 | 2407.2 | A' | 808 | 6.9 | | CO ₂ antisymmetric stretch |
| 1369.2 | Σ _g | 0 | 1373.5 | A' | 1 | 4.3 | | CO2 symmetric stretch |
| 1362.6 | E' | 190 | 1367.2 | A'' | 183 | 4.6 | 13.1 | SO ₃ antisymmetric stretch |
| | | | 1363.8 | A' | 185 | 1.2 | 10.2 | |
| 1044.1 | A' ₁ | 0 | 1046.6 | A' | 0 | 2.4 | | SO ₃ symmetric stretch |
| 673.8 | Π _u | 30 | 670.7 | A' | 29 | -3.1 | | CO ₂ bending |
| | | | 668.8 | A'' | 29 | -5.0 | | |
| 507.9 | E' | 25 | 509.2 | A'' | 24 | 1.3 | 4.4 | SO ₃ in-plane bend |
| 507.9 | E' | 25 | 508.7 | A' | 23 | 0.8 | 4.4 | SO ₃ in-plane bend |
| 475.7 | A'' ₂ | 32 | 473.1 | A' | 55 | -2.6 | -1.9 | SO ₃ out-of-plane bend |
| | | | 84.6 | A' | 0 | | | Frustrated translations and rotations |
| | | | 69.2 | A'' | 0 | | | |
| | | | 58.8 | A' | 1 | | | |
| | | | 14.0 | A' | 0 | | | |
| | | | 6.5 | A'' | 0 | | | |

upon normal mode analyses using the ab initio calculated harmonic force fields. As can be seen, there is a good agreement, although the calculated shift of the very anharmonic hydrogen bonded O–H stretching mode is too large. The vibrational frequencies from an MP2/aug-cc-pVDZ calculation differ slightly from the B3LYP/aug-cc-pVTZ results. However, the wave-number shifts upon complexation and the normal mode pictures are almost the same. The (CO₂)·(SO₃) complex is weak and a priori no structure is obvious. To probe the potential surface, calculations were carried out for several distinct structures. The results are summarized in Table 5 showing that there is only one single true energy minimum, for the structure reproduced in Fig. 3B and that the energy surface is very shallow. However, it is clear from the calculations that the complex bonding is O₃S···OCO. The CP-corrected bonding energy and enthalpy is calculated as -6.2 and -2.3 kJ mol⁻¹, respectively, at the B3LYP/aug-cc-pVTZ level, the correction being -0.6 kJ mol⁻¹. The other levels of calculations gave essentially the same values. However, the CP-corrections were larger for the smaller basis sets. The different calculations gave slightly different minimum

energy structures, the difference being, not surprisingly, only the angle between the O=C=O chain and the SO₃ plane. The calculated vibrational modes and infrared intensities of the complex and the isolated monomers are compared in Table 6. The Table also includes an interpretation of the vibrations based upon normal mode analyses using the ab initio calculated harmonic force fields as well as the observed and calculated shifts upon complexation. The observed spectral shifts of the antisymmetric SO₃ stretching modes, although in the same direction, are considerably larger than the calculated values. Quite possibly, for the shallow potential surface characterizing this complex, the matrix environment affects the sensitive parameter of the angle between the O=C=O chain and the SO₃ plane. Such effect would decrease the separation between the C atom of CO₂ and the nearest O atom of SO₃ and thus increase the secondary interaction between them.

6. Summary

1:1 (CO₂)·(H₂SO₄) and (CO₂)·(SO₃) complexes

were trapped in solid argon and found to be formed mostly during the depositions of the gaseous mixtures. The wavenumber values of their characteristic vibrational modes were determined. From the relative shifts of these modes, an order of bonding strengths could be deduced: $\text{N}_2 < \text{CO}_2 < \text{NO} \sim \text{N}_2\text{O}_2 < \text{CO}$ for the $(\text{L}) \cdot (\text{H}_2\text{SO}_4)$ complexes and $\text{N}_2 < \text{CO}_2 < \text{CO}$ for the $(\text{L}) \cdot (\text{SO}_3)$ complexes. The spectra indicate a $\text{O}=\text{C}=\text{O} \cdots \text{HO}$ bond for the 1:1 $(\text{CO}_2) \cdot (\text{H}_2\text{SO}_4)$ complex and a main $\text{O} \cdots \text{S}$ interaction and a secondary $\text{C} \cdots \text{O}$ interaction for the 1:1 $(\text{CO}_2) \cdot (\text{SO}_3)$ species.

References

- [1] D.R. Hanson, E.R. Lovejoy, *Science* 267 (1995) 1326.
- [2] A. Givan, A. Loewenschuss, C.J. Nielsen, *J. Chem. Soc. Faraday Trans.* 94 (1998) 827.
- [3] A. Givan, A. Loewenschuss, C.J. Nielsen, *J. Mol. Struct.* 509 (1999) 35.
- [4] A. Givan, L.A. Larsen, A. Loewenschuss, C.J. Nielsen, *J. Chem. Soc. Faraday Trans.* 94 (1998) 2277.
- [5] A. Givan, A. Loewenschuss, C.J. Nielsen, *Phys. Chem. Chem. Phys.* 1 (1999) 37.
- [6] A. Givan, A. Loewenschuss, C.J. Nielsen, *J. Phys. Chem.* 104 (2000) 3441.
- [7] L. Schriver, D. Carrere, A. Schriver, K. Jaeger, *Chem. Phys. Lett.* 181 (1991) 505.
- [8] T.L. Tso, E.K.C. Lee, *J. Phys. Chem.* 88 (1984) 2781.
- [9] M.J. Frisch, G.W. Trucks, H.B. Schlegel, G.E. Scuseria, M.A. Robb, J.R. Cheeseman, V.G. Zakrzewski, J.A. Montgomery, Jr., R.E. Stratmann, J.C. Burant, S. Dapprich, J.M. Millam, A.D. Daniels, K.N. Kudin, M.C. Strain, O. Farkas, J. Tomasi, V. Barone, M. Cossi, R. Cammi, B. Mennucci, C. Pomelli, C. Adamo, S. Clifford, J. Ochterski, G.A. Petersson, P.Y. Ayala, Q. Cui, K. Morokuma, D.K. Malick, A.D. Rabuck, K. Raghavachari, J. B. Foresman, J. Cioslowski, J. V. Ortiz, A. G. Baboul, B. B. Stefanov, G. Liu, A. Liashenko, P. Piskorz, I. Komaromi, R. Gomperts, R.L. Martin, D.J. Fox, T. Keith, M.A. Al-Laham, C.Y. Peng, A. Nanayakkara, C. Gonzalez, M. Challacombe, P.M.W. Gill, B. Johnson, W. Chen, M.W. Wong, J.L. Andres, C. Gonzalez, M. Head-Gordon, E.S. Replogle, J.A. Pople, Gaussian Inc., Pittsburgh, PA, 1998.
- [10] A.D. Becke, *J. Chem. Phys.* 98 (1993) 5648.
- [11] F.B. Van Duijneveldt, J.G.C.M. Van Duijneveldt-van, J.H. Van Lenthe, *Chem. Rev.* 94 (1994) 1873.
- [12] G.O. Soerensen, Chemical Institute, University of Copenhagen.
- [13] R.M. Bentwood, A.J. Barnes, W.J. Orville-Thomas, *Mol. Spectrosc.* 84 (1980) 391.
- [14] T.L. Tso, E.K.C. Lee, *J. Phys. Chem.* 89 (1985) 1612.
- [15] T.L. Tso, E.K.C. Lee, *J. Phys. Chem.* 89 (1985) 1618.
- [16] A. Givan, A. Loewenschuss, C.J. Nielsen, unpublished results.
- [17] P. Beichert, O. Schrems, *J. Phys. Chem. A* 102 (1998) 10540.
- [18] G.C. Pimentel, R.D. Sprately, *Chemical Bonding Clarified Through Quantum Mechanics*, Holden-Day, 1969.
- [19] W.M. Huo, *J. Chem. Phys.* 43 (1965) 624.
- [20] J. Sadlej, B. Rowland, J.P. Devlin, V. Buch, *J. Chem. Phys.* 102 (1995) 4804.
- [21] A. Givan, A. Loewenschuss, C.J. Nielsen, *J. Chem. Soc. Faraday Trans.* 92 (1996) 4927.
- [22] J. Lundell, M. Rasanen, *J. Phys. Chem.* 99 (1995) 14301.
- [23] A.J. Barnes, E. Lasson, C.J. Nielsen, *Trans. Faraday Soc.* 91 (1995) 3111.
- [24] K.I. Peterson, W.J. Klemperer, *J. Chem. Phys.* 80 (1984) 2439.
- [25] B. Jonsson, G. Karlstrom, H. Wennerstrom, *Chem. Phys. Lett.* 30 (1975) 58.
- [26] F.A. Cotton, G. Wilkinson, *Advanced Inorganic Chemistry, A Comprehensive Text*, 5th ed., Wiley, New York, 1988 p. 517.